Plant Pathology (2009) **58**, 370–377 Doi: 10.1111/j.1365-3059.2008.01954.x

Effect of plot geometry on epidemic velocity of wheat yellow rust

K. E. Sackett* and C. C. Mundt

Botany and Plant Pathology Department, 2082 Cordley Hall, Oregon State University, Corvallis, OR 97331-2902 USA

The size and shape of field plots can impact on both the cost and outcome of epidemiological experiments. In previous studies, epidemic velocity of yellow rust (caused by *Puccinia striiformis* f.sp. *tritici*) on wheat (*Triticum aestivum*) has been examined in long, narrow plots (6·1 m by 73–171 m). The present study compares spread in square, 61 × 61 m plots versus narrow, 6·1 × 61 m plots at two locations. The objective was to test whether plot shape has a substantial impact on spatiotemporal spread of yellow rust. Velocity increased curvilinearly with time for both plot shapes and at both locations. Curves of epidemic velocity versus time were nearly identical in square versus narrow plots in both the upwind and downwind directions. Contrary to expectation based on simulations, the results did not indicate faster disease spread in square plots, though the plot sizes studied may be beyond that at which there is a rapid change of disease increase with increasing plot area. Velocity also increased curvilinearly in all eight compass directions of the square plots. Results indicate that narrow plots, which are substantially less costly than equidimensional plots, may be justified for studying the spatiotemporal spread of wheat yellow rust and other diseases with similar epidemiological characteristics.

Keywords: anisotropy, epidemiology, *Puccinia striiformis* f.sp. *tritici*, *Triticum aestivum*

Introduction

Epidemiological field experiments can be costly and logistically difficult, primarily because large tracts of land may be required in order to observe the spatial progress of an epidemic over many pathogen generations. An important goal, therefore, is to minimize the amount of land required for such studies, while retaining their relevance to 'real world' epidemics. In some cases, spread in a particular direction may be of most interest. For instance, in the case of windborne pathogens, disease is likely to spread fastest in the direction of the strongest winds. Also, if spread is equal in all directions, examination of disease along one transect may be sufficient to understand the dynamics in the other directions. Nonetheless, in the landscape, natural epidemics spread in all directions, and so it is important to understand differences, if any, between one- and two-dimensional spread.

Square plots allow researchers to follow disease progress in multiple directions, but rapidly become unfeasible as they become larger, since their areas increase as the square of plot length. In contrast, planting long, narrow plots is a much more efficient use of available land. Plot (or field) shape, however, may affect disease dynamics. Models suggest that square plots (Paysour & Fry, 1983) and fields (Waggoner, 1962; Fleming *et al*., 1982) are likely to support higher disease levels than elongated ones of the same area, and that orienting elongated plots perpendicular to prevailing winds may suppress epidemic progression (Waggoner, 1962; Fleming *et al*., 1982). Plot size may also have an effect. In square configurations, severity of disease was greater for large plots than for small plots in the field (Paysour & Fry, 1983; Bowen *et al*., 1984; Mundt *et al*., 1996); the same was true in computer simulations (Paysour & Fry, 1983; Mundt & Brophy, 1988). Other models have predicted similar impacts of field size on disease (Waggoner, 1962; Fleming *et al*., 1982). These results presumably were caused by a larger proportion of spores being retained within larger plots. However, on a regional scale van der Plank (1948, 1949, 1960) argued that, given constant total area of a crop within a region, large fields would be advantageous since they would impede spread among fields.

The current study addresses plot geometry in the context of the velocity of epidemic spread, a topic of significant current and historical interest in plant disease epidemiology (Zadoks, 2001; Scherm *et al*., 2006). *Velocity* and *epidemic velocity* as used here are equivalent to the term *isopathic velocity*, which was introduced by Berger & Luke (1979) to quantify disease spread in focal plant epidemics, an *isopath* being defined as a contour in space of constant disease level. As a focal epidemic progresses,

*E-mail: sackettk@science.oregonstate.edu

Published online 14 October 2008

isopaths expand outward from the focus (the site of initial infection). The rate of movement of an isopath in a particular direction is its *velocity*, expressed in units of distance per time (e.g. m week^{-1}). Earlier mathematical studies, supplemented with limited field data, suggested that epidemics increase as travelling waves, i.e. waves of constant velocity (Minogue & Fry, 1983; Heesterbeek & Zadoks, 1987; van den Bosch *et al*., 1988a,b,c). Ferrandino (1993) later developed a mechanistic rationale for dispersive epidemic waves, which expand with increasing velocity. Evaluation of both historical (Scherm, 1996) and experimental (Frantzen & van den Bosch, 2000) data sets lent support to the existence of dispersive epidemic waves, but the evidence was not considered to be definitive by the authors. In the latter case, plots 0·9 × 97 – 99 m were used in an attempt to capture disease dynamics at large distances without requiring large amounts of land. More recently, epidemic velocity of wheat yellow rust (caused by *Puccinia striiformis* f.sp. *tritici*) was examined in 6·1 m wide plots ranging in length from 73 to 171 m (Cowger *et al*., 2005; Sackett & Mundt, 2005a). Epidemic velocity showed a consistent pattern of increasing exponentially with time and linearly with distance when measured in either the downwind or upwind direction, regardless of the isopath level used to measure velocity. Furthermore, mixing a susceptible wheat cultivar with an immune one suppressed the increase of velocity in time and space.

Common sense and preliminary computer simulations suggest that epidemics may proceed at least slightly faster in square plots as compared to rectangular ones of the same length because there are more infected plants producing spores in square plots. A qualitative effect of plot shape on epidemic spread would be of much greater concern, e.g. if dispersive waves were detected with one plot shape and travelling waves with another. Thus, the objective of the current study is to compare the spread of wheat yellow rust from artificially inoculated foci in square field plots with spread in rectangular plots of the same length. The square plots also allowed analysis of whether direction of measurement has an influence on patterns of epidemic spread.

Materials and methods

Field plots

Field experiments took place at two locations in Oregon, USA during the 2003–2004 winter wheat growing season: the Central Oregon Agricultural Research Center in Madras, and the Hermiston Agricultural Research and Extension Center. Weather stations at both sites recorded wind, temperature, rainfall, and other data on an hourly basis. The Madras site is located at the eastern base of the Cascade Mountains, at an elevation of 742 m; the Hermiston site is 193 km to the northeast, on the plains of the Columbia River basin (elev. 191 m). The Hermiston site has sandier soil – fine sandy loam as opposed to loam at the Madras site – and experienced slightly warmer temperatures during the course of these experiments (mean 12·0°C, compared to 10·7°C in Madras). Strong winds are common at both sites: average daily peak windspeeds during the experiments were 9·0 m s^{-1} in Hermiston and 12·1 m s^{-1} in Madras. However, the strongest winds during the spring of 2004 in Hermiston were almost always from the west to southwest; strong winds in Madras had more directional variation, though they were almost never from the north or east. Weaker winds (< 2 m s^{-1}) came most often from the west or southeast in Hermiston, from the northeast to southeast in Madras.

Experimental plots were planted in the autumn (25 September in Madras; 14 October in Hermiston) with winter wheat cv. Jacmar, which is highly susceptible to *P. striiformis*. At each location, there were two replicates of two plot shape treatments: narrow plots were 6·1 × 61·0 m, with the long axis running west to east; square plots were 61·0 × 61·0 m. Plots were separated from one another as much as possible, with cv. Stephens (not susceptible to the rust race used) filling the remainder of each field, including a minimum 6·1 m wide buffer zone between the plots and the edges of the fields (Fig. 1). Plots were planted using a 6-row, 1·52 m wide seed drill, at a rate of 323 seeds m^{-2}. Fertilizer and pesticides were applied according to standard local commercial practice. Regular overhead irrigation began in early spring at a frequency of once per week in Madras, and three to five times per week in Hermiston.

Inoculation

A 1·52 m^2 area in each plot was inoculated in the spring (2 March in Hermiston; 17 March in Madras) with *P. striiformis* race PST-5, to which commercial cultivars grown in the area are resistant. At inoculation time, plants were at growth stage 4 to 5 on the Feekes scale (Large, 1954). Areas to be inoculated (foci) were first sprayed with water to improve adhesion of spores and to encourage germination. For each plot, 0·25 g of fresh urediniospores mixed with 2 g talc were dusted uniformly onto the plants. Foci were covered with black plastic sheets overnight to maintain humidity.

Disease assessment

Weekly disease assessments were made at each site, beginning with the first appearance of sporulating rust lesions, and continuing until plants began to senesce at the end of the season. In each narrow plot, assessments were done in the focus, at 6·1 m intervals east and west of the focus, and at 1·5 and 3·0 m from the centre of the focus. Since the initial disease foci were placed slightly upwind of the centre of the plots, there were more assessment locations east (downwind) of the foci. Square plots were additionally assessed at similar intervals along transects north, south, and in the four ordinal directions from the focus (Fig. 2). Along the ordinal transects, the closest assessment point was at 3·0 m, since a 1·5 m assessment would have overlapped with the corner of the focus. A wire flag was placed at each assessment point. The last

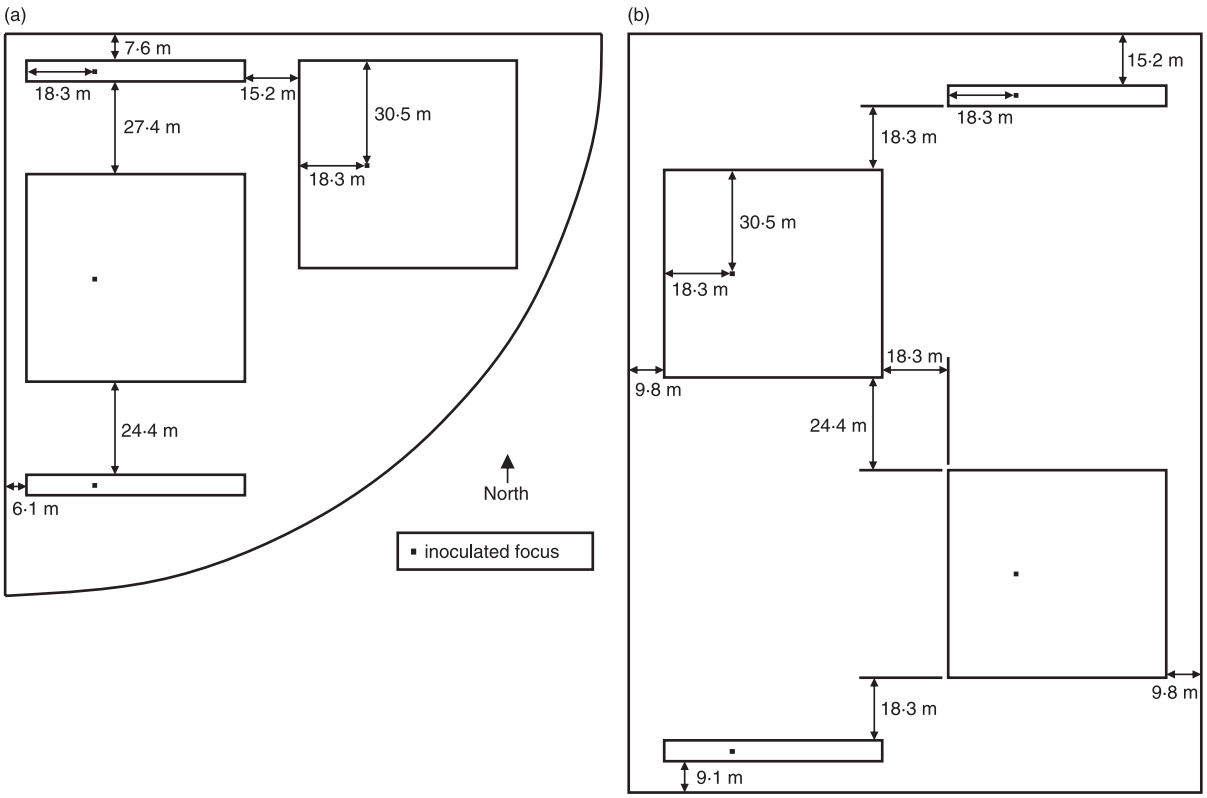

Figure 1 Plot layouts for wheat yellow rust experiments in (a) Hermiston and (b) Madras, OR, in 2004. Square (61·0 m × 61·0 m) and narrow (61·0 × 6·1 m) plots were planted to the susceptible cv. Jacmar; remainder of each field was planted to the non-susceptible cv. Stephens. Inoculated foci measured 1·52 × 1·52 m. Prevailing winds at both sites are generally from the west.

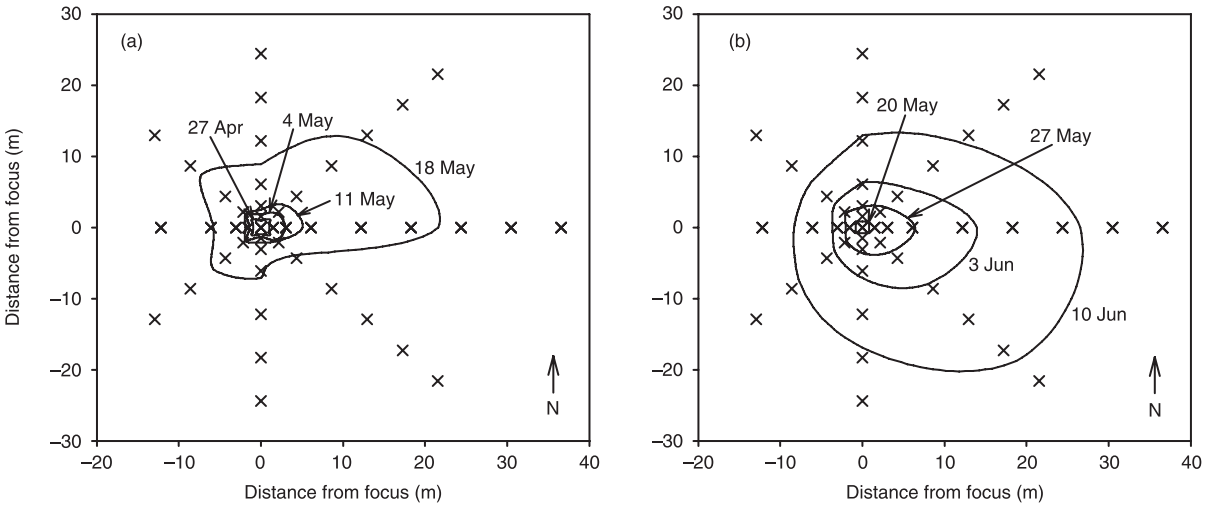

Figure 2 Field epidemics of wheat yellow rust in square plots during spring 2004. Plot (a) shows the estimated location of the 10% severity isopath based on weekly observations in Hermiston; (b) shows the 20% isopath in Madras. Isopath locations are based on mean severity over two replications at each site. Assessment locations are marked by 'x'. X also indicates the approximate size of inoculated areas and assessed areas. Field plots measured 61·0 × 61·0 m (see Fig. 1).

flag in each direction was at least 6·1 m from the edge of the plot. Total disease severity (percentage leaf area affected by yellow rust) at each flag was estimated visually by two observers. Each observer was assigned half of a 1·5 m^2 area with the marker flag at the centre, and determined an average score based on perusal of the entire assigned area; the average of the two readings was recorded.

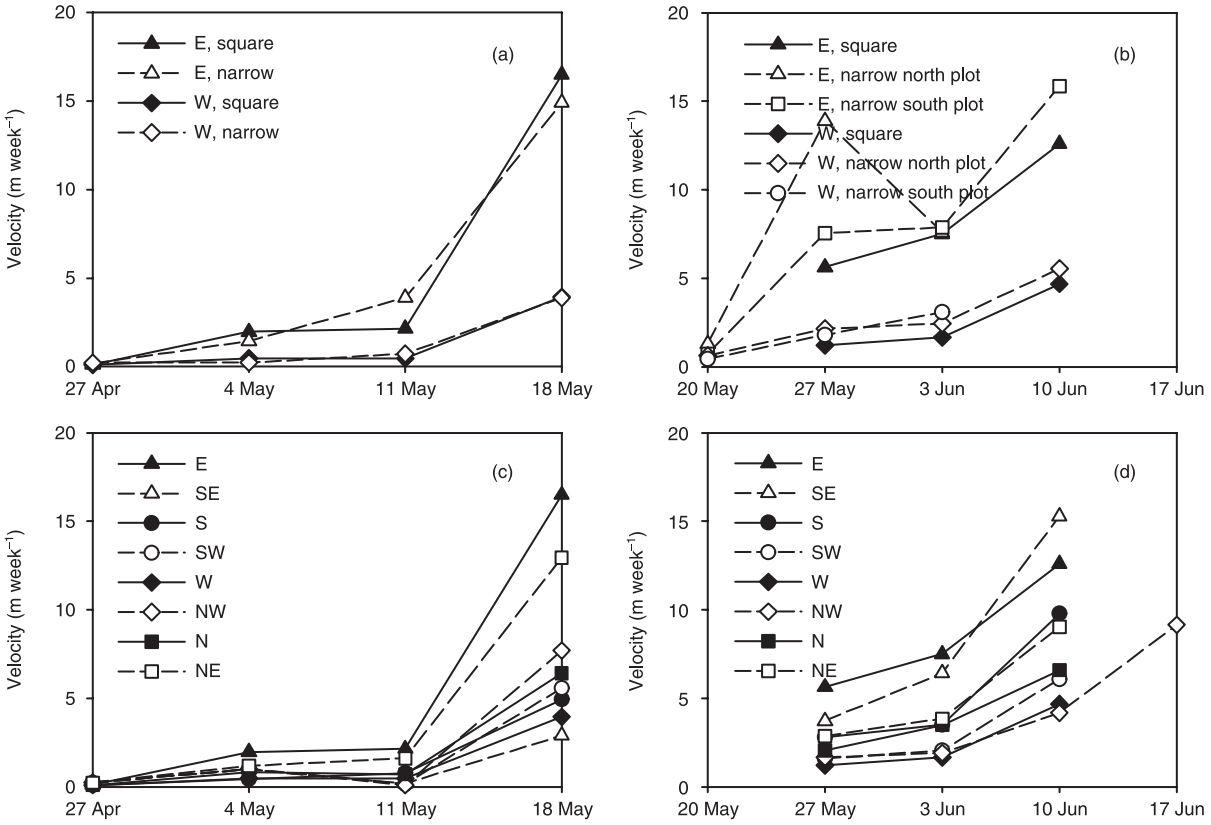

Figure 3 Isopathic velocity of expansion from initial focus of infection in field epidemics of wheat yellow rust in (a, c) Hermiston (10% isopath), and (b, d) Madras (20% isopath) during spring 2004. Velocities were calculated from severities averaged over two replicate plots, except Madras narrow plots, which are shown individually. Plots (a) and (b) represent upwind (W) and downwind (E) velocities for both square and narrow plots; (c) and (d) represent square field plots only.

Data analysis

For each location, a single isopath (severity) level was chosen for analysis such that the maximum number of assessment dates could be included. In Hermiston, the 10% severity isopath was chosen; in Madras the 20% isopath. Previous field and computer simulation studies have indicated that, for a given epidemic, the choice of isopath does not substantially affect velocity curve shapes (Cowger *et al.*, 2005; Sackett & Mundt, 2005b).

In order to compare the two plot shape treatments, incorporating information on variability among plots, velocity was calculated for each plot separately. Isopath locations along the east and west transects were estimated for each assessment date. Where the chosen isopath level was between two assessment locations, linear interpolation was used to estimate its location in the field. The velocity (m week^{-1}) assigned to each date was the distance the isopath had travelled between that week and the previous week. For those dates where the isopath was located within all four plots (i.e. the velocity could be estimated), a two-tailed paired *t*-test was performed to compare the treatments. In Hermiston, this analysis was possible for four dates (27 April, 4 May, 11 May and 18 May); in Madras, only 27 May and 3 June could be used. A total of twelve *t*-tests resulted (six dates × two directions).

For the purpose of illustrating trends in epidemic velocity over time (Fig. 3), isopath locations in each transect direction were calculated based on the mean severity of two replicate plots. This allowed the inclusion of more assessment dates, giving a clearer picture of how the epidemics developed over time. There were instances where an isopath had moved past the margins of one plot, making the velocity of that isopath impossible to calculate, while at the same time the corresponding plot still contained that isopath. Averaging severities before calculating velocity allowed some of these data points to be included in Fig. 3.

To examine the relationship between disease spread and wind direction and strength, wind speed and direction data were compiled for the effective dispersal period of the epidemic. This period began one latent period after inoculation, when lesions on plants in the inoculated foci began to produce spores. It ended one latent period before the last assessment date: spores produced after this point did not produce visible disease by the last assessment, and thus did not contribute to observed disease levels. Hourly

wind speed readings were summed over this period for each of the eight transect directions to give cumulative wind speeds for the epidemic. For each location, latent periods were estimated based on degree-hour calculations (Shrum, 1975). The distance of the relevant isopath from the centre of the inoculated focus was regressed on cumulative wind speed for each location.

Simulations

A series of computer simulations was performed using the spatially explicit model EPIMUL (Zadoks & Kampmeijer, 1977; Sackett & Mundt, 2005b) to assess the risk of interplot interference in the field experiments. The experiment in Hermiston served as the basis for these simulations; because the plot layout (Fig. 1a) was more compact there than in Madras (Fig. 1b), the probability of spore travel between plots was presumed to be greater. Simulation parameters were largely identical to those used previously to emulate a field epidemic at the Hermiston site in 2002 (Cowger *et al*. 2005; Sackett & Mundt 2005b, baseline simulation). In particular, latent period was 14 days, infectious period was 11 days, lesion growth rate was 0·25 per day, and daily multiplication factor was 5. The first generation disease levels in the inoculated foci were lower in the field in 2004 than in 2002, so the simulated inoculation level was correspondingly lower: 6000 spores per focus, rather than 115 000. Dispersal was modelled using the modified power law:

$$y = a(x + c)^{-b}$$

with $a = 118{\cdot}15$, $b = 2{\cdot}41$, $c = 0{\cdot}543$ to the west, and $a = 6111{\cdot}7$, $b = 2{\cdot}0$, and $c = 2{\cdot}57$ to the east. y is the number of effective spores deposited at distance x from the source plant. The eastern dispersal gradient was adjusted to be less steep than in the simulation of the 2002 epidemic, so that disease levels at the end of the epidemic closely resembled those observed in the field at the last assessment.

Three simulations were run: one with susceptible plants laid out in four plots, as in the field experiment (Fig. 1a), each plot being inoculated in a single location; one with only a single square plot present; and one with a single narrow plot present. Velocity of the 10% severity isopath was calculated for each plot. Comparison of disease spread in the solo plots versus plots of the same shape when other plots were present gives an indication of the potential for interplot interference.

For ease of interpretation, the simulated epidemics were 'assessed' on simulation days corresponding to assessment days in the field. The correct simulation day was calculated by estimating the fractional number of latent periods completed at each assessment date, according to temperatures recorded hourly at the field site (Shrum, 1975). For example, on 27 April, 3·2 latent periods (pathogen generations) had elapsed since the date of inoculation, corresponding to day 54 of the simulations.

The daily multiplication factor and steepness of the dispersal gradient were varied in several ways in preliminary simulations, in an attempt to reproduce the field epidemics (results not shown). Differences between square and narrow plots varied among these simulations, but spread was always slower in narrow plots than in square ones (unlike in the field epidemics). However, in no case was there evidence for substantial interplot interference.

Table 1 Comparison of velocity (m week^{-1}) of wheat yellow rust in square versus narrow plots at individual assessment dates upwind (West) and downwind (East) of the inoculated foci, based on two replicates at each site. Velocities were calculated for the 10% isopath in Hermiston and the 20% isopath in Madras

		Difference[a]		*P*-value[b]	
Site	Date	East	West	East	West
Hermiston	27 April 2004	–0·12	–0·23	0·611	0·503
Hermiston	4 May 2004	0·77	0·45	0·061	0·027
Hermiston	11 May 2004	–2·12	–0·18	0·296	0·047
Hermiston	18 May 2004	1·04	–0·56	0·682	0·438
Madras	27 May 2004	–4·35	–0·22	0·418	0·726
Madras	3 Jun 2004	–0·43	–1·06	0·744	0·035

[a]Mean velocity in square plots minus mean velocity in narrow plots.
[b]*P*-values resulting from two-tailed paired *t*-tests comparing velocity in square versus narrow plots.

Results

Narrow versus square plots

In both locations, epidemic velocity was qualitatively and quantitatively similar in square and narrow plots (Fig. 3a,b). That is, not only did velocity increase more than linearly over time in all cases, but the magnitude of velocity was also similar in plots of different shape. Nine of the twelve two-tailed paired *t*-tests comparing velocity (m/week) in square versus narrow plots at each assessment date in both upwind and downwind directions detected no significant difference ($P > 0{\cdot}05$) (Table 1). Two of the remaining comparisons were for the upwind (west) Hermiston data, in consecutive weeks. The magnitudes of both differences were quite small (Table 1, Fig. 3a), and in fact were of opposite signs, indicating no tendency for one treatment or the other to effect greater epidemic velocity. The difference between velocity in square and narrow plots in the downwind direction (east) in Hermiston also alternated sign from week to week (Table 1, Fig. 3a), so it is unlikely that the borderline *P*-value from the 4 May *t*-test has any practical significance. The third *t*-test that showed statistical significance was for 3 June in Madras, west ($P = 0{\cdot}035$) (Table 1). Again here, the size of the difference was small (1·06 m week^{-1}).

The similarity between treatments was particularly striking in the Hermiston plots, where velocity curves for the two plot shapes were nearly indistinguishable, both upwind and downwind of the initial disease focus (Fig. 3a). Interpretation of the Madras data (Fig. 3b) was

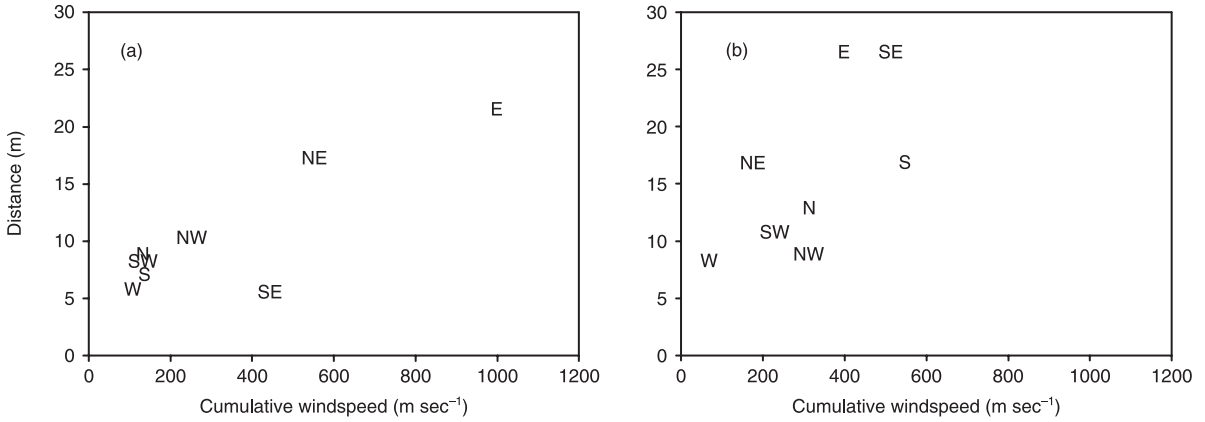

Figure 4 Relationship between wind and disease spread in field epidemics of wheat yellow rust. Distance of isopath from the centre of inoculated focus in eight transect directions at the last assessment date is plotted against cumulative wind speed (sum of hourly observations in each of eight downwind directions) during dispersal (from one latent period after inoculation until one latent period before last disease assessment, based on degree-hour calculations (Shrum, 1975)). Plot (a) shows the 10% severity isopath in Hermiston on 18 May 2004; (b) shows the 20% isopath in Madras on 10 Jun 2004.

complicated by the presence of uneven environmental conditions: overspray from irrigation of an adjacent field caused the northernmost narrow plot to be more lush and conditions more conducive to rapid disease increase than in the other three plots. Downwind epidemic velocity spiked early in the season in this plot, and by 10 June, severity at all points east of the focus had exceeded 20%, so that the location of the 20% isopath could not be estimated. Downwind velocity in the southern narrow plot was similar to the square plots. Importantly, velocity increased more than linearly in all cases except the northernmost narrow plot in Madras.

Within square plots

The shape of the epidemic velocity curves for the square plots at both Hermiston and Madras was similar along all eight transects, increasing more than linearly in each case (Fig. 3c,d). As expected, velocity increased faster toward the east than the west, reflecting the predominant wind direction at these locations. The wind during the effective dispersal period for the two epidemics correlated well with disease spread, both in terms of epidemic velocity and total distance travelled by an isopath. In Hermiston, wind, velocity and distance travelled were greatest to the east and northeast; in Madras, they were greatest to the east, southeast and south (Figs 2–4). The relationship between cumulative wind speed and distance travelled was strong (P = 0·006 in Hermiston, P = 0·08 in Madras for the null hypothesis that the slope of the regression line was zero; Fig. 4). As a result of this preferential spread, the shape of the expanding foci became more oblong as the epidemics progressed (Fig. 2).

Simulations

Simulations indicated a small increase in epidemic velocity due to the presence of nearby plots also carrying disease

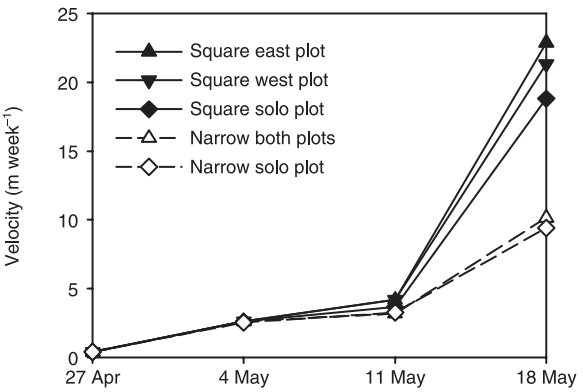

Figure 5 Effect of interplot interference in simulated epidemics. Simulations were performed based on a wheat yellow rust field experiment in Hermiston, OR in 2004 (see Fig. 1a for plot configuration) using EPIMUL (Zadoks & Kampmeijer, 1977; Sackett & Mundt, 2005b) with the following model parameters: latent period 14 days, infectious period 11 days, lesion growth rate 0·25 per day, daily multiplication factor 5, inoculation level 6000 spores per focus, and dispersal according to a modified power law, $y = a(x + c)^{-b}$, with a = 118·15, b = 2·41, c = 0·543 to the west, and a = 6111·7, b = 2·0, and c = 2·57 to the east. Graph shows velocities of the 10% severity isopath downwind (east) of the inoculated focus at times corresponding to assessment dates for the field experiment. Triangles (▲, ▼, △) indicate results from full simulation of the field experiment, with two square and two narrow plots, each inoculated at a single location. Results were identical for the two narrow plots. Diamonds (◆, ◇) are results for two further simulations, in which only a single plot – square or narrow – was present.

(Fig. 5). In narrow plots, the difference in velocity was negligible: less than a metre per week, even at the height of the epidemic. For square plots, the difference was 3·3 m week^{-1} at the end of the epidemic, still quite small compared to the predicted difference between square and

narrow plots (11·9 m week^{-1}), which, as noted above, did not materialize in the field. The full simulation predicted a slight difference between the two square plots: the downwind (east) plot's velocity was 1·52 m week^{-1} greater than the velocity in the upwind plot at the last assessment date. The relationship was reversed in the field experiment: the downwind plot's final velocity was smaller by 3·16 m week^{-1} (differences between square plots were far smaller for the other dates). This difference appears not to be a result of interplot interference. The simulation pointed to the downwind plot as the most likely to be influenced by inoculum travelling from other plots. On the other hand, if crosswind (north-south) and/or upwind (west) dispersal were stronger than modelled in this simulation, the most centrally-located plot might be more susceptible to interplot interference. However, this latter hypothesis is not supported by the field data: north-south transect severities were lower in the field than in simulations.

Discussion

Spatial and temporal progression of the field epidemics in this study was consistent with the results of previous studies of wheat yellow rust (Emge & Shrum, 1976; Cowger *et al*., 2005). Isopaths moved away from inoculated foci with velocities that increased with time, contradicting the prediction of constant velocity by travelling wave models (Minogue & Fry, 1983; Heesterbeek & Zadoks, 1987; van den Bosch *et al*., 1988a,b). In the current study, acceleration of isopaths away from foci was observed regardless of the direction of the assessed transect, and regardless of whether the plot was square or narrow. This result validates previous use of narrow plots to investigate the spatio-temporal spread of plant disease (Frantzen & van den Bosch, 2000; Cowger *et al*., 2005), a practice that makes much more efficient use of field space than using only equidimensional plots. For example, Cowger *et al*. (2005) were able to plant six narrow plots where only two square ones would have fit. Not only was replication of treatments possible, but the increased ratio of buffer area to plot area reduced the possibility of interplot interference. The fact that disease spread in a qualitatively similar manner in all transect directions suggests that, although more dispersal events may occur in some directions, the physical mechanisms involved in spore dispersal are the same in all directions.

The lack of a detectable difference between square and narrow plots was unexpected. Although the power of the *t*-tests used to compare the treatments was low, given only two replicates per site, the size of the expected treatment effect (Fig. 5) was such that, had it materialized in the field, it should have been discernable. It is still possible that some effect of plot size or shape on disease spread existed, but that it was too small to detect. In any case, the effect appears to be too small to have practical significance.

This result differs from some other published studies of plot size and shape. The lack of an effect of plot area on disease may be explained by the difference in plot size between this study and others. A series of square plots ranging from 0·36 to 24·0 m^2 for wheat yellow rust (Mundt *et al*., 1996), 0·81 to 29·2 m^2 for potato late blight (Paysour & Fry, 1983), and 1 to 5000 m^2 for a study of *Valdensia heterodoxa* on *Vaccinium myrtillus* (Strengbom *et al*., 2006) indicate an initial increase in disease levels as plot area increases, with the response levelling off at the larger plot sizes. The smallest plot in the current study (372 m^2) was substantially larger than the largest plot size in two of these studies (Paysour & Fry, 1983; Mundt *et al*., 1996) and within the range of plot size at which disease levels became asymptotic in the *Vaccinium* study. Severity of brown rust on wheat was generally lower in small (4 m^2) than in larger (16 m^2) plots (Bowen *et al*., 1984), but both plot sizes were substantially smaller than those used in the current study. It thus appears that, when a certain plot area is reached, there may either be no effect of further increases or else a very large change of plot size may be required to obtain an observable effect. These two possibilities cannot be distinguished for the current study, as there was only a 10-fold difference in area between the two plot sizes. Also, in this experimental design, plot size was confounded with plot shape. Others have reported an effect of field shape when area was held constant (Waggoner, 1962; Fleming *et al*., 1982), but no field validation was available in those studies. It is known that choosing the correct parameters for large-scale dispersal is difficult (Sackett & Mundt, 2005a), but can be crucial to such modelling efforts.

As in other studies of wheat yellow rust (Emge & Shrum, 1976; Soubeyrand *et al*., 2007) disease spread in square plots was distinctly anisotropic. Unsurprisingly, disease spread correlated strongly with wind speed and direction. The presence of prevailing winds tended to elongate the expanding focus in the downwind direction. However, the shape of the focus is not perfectly predicted by wind alone, as successful infection requires a favorable microenvironment, which will not be present for all dispersal events.

Interplot interference is of significant concern in many epidemiological experiments, but is the result of complex interactions among dispersal gradients, plot size, plot shape, and distance between plots (Paysour & Fry, 1983). In the current study, efforts were made to minimize spore transfer between plots by arranging them as far apart in the field as possible, while keeping the plot sizes large enough that meaningful velocity data could be collected. Spatially explicit simulations of disease spread for the more compact layout (in Hermiston) suggested that although some spore exchange between plots was likely, the magnitude of the effect on velocity was too small to detect in the field (Fig. 5).

At the spatial scales studied, the spread of wheat yellow rust was qualitatively and quantitatively similar in narrow as compared to square plots. The same is likely to be true of other systems with similar epidemiological characteristics, thus allowing more economical field designs to study the spatiotemporal spread of disease rather than the use of equidimensional plots.

Acknowledgements

Many thanks to the staff of the Central Oregon Agricultural Research Center in Madras and the Hermiston Agricultural Research and Extension Center for expert help with field operations. This work was supported by award 97-353034537 from the USDA National Research Initiative Competitive Grants Program and award 052756 from the NSF/NIH Ecology of Infectious Diseases Program.

References

Berger RD, Luke HH, 1979. Spatial and temporal spread of oat crown rust. *Phytopathology* **69**, 1199–201.

van den Bosch F, Frinking HD, Metz JAJ, Zadoks JC, 1988a. Focus expansion in plant disease. III: two experimental examples. *Phytopathology* **78**, 919–25.

van den Bosch F, Zadoks JC, Metz JAJ, 1988b. Focus expansion in plant disease. I: the constant rate of focus expansion. *Phytopathology* **78**, 54–8.

van den Bosch F, Zadoks JC, Metz JAJ, 1988c. Focus expansion in plant disease. II: realistic parameter-sparse models. *Phytopathology* **78**, 59–64.

Bowen KL, Teng PS, Roelfs AP, 1984. Negative interplot interference in field experiments with leaf rust of wheat. *Phytopathology* **74**, 1157–61.

Cowger C, Wallace LD, Mundt CC, 2005. Velocity of spread of wheat stripe rust epidemics. *Phytopathology* **95**, 972–82.

Emge RG, Shrum RD, 1976. Epiphytology of *Puccinia striiformis* at five selected locations in Oregon during 1968 and 1969. *Phytopathology* **66**, 1406–12.

Ferrandino FJ, 1993. Dispersive epidemic waves. I: focus expansion within a linear planting. *Phytopathology* **83**, 795–802.

Fleming RA, Marsh LM, Tuckwell HC, 1982. Effect of field geometry on the spread of crop disease. *Protection Ecology* **4**, 81–108.

Frantzen J, van den Bosch F, 2000. Spread of organisms: can travelling and dispersive waves be distinguished? *Basic and Applied Ecology* **1**, 83–91.

Heesterbeek JAP, Zadoks JC, 1987. Modelling pandemics of quarantine pests and diseases: problems and perspectives. *Crop Protection* **6**, 211–21.

Large EC, 1954. Growth stages in cereals, illustration of the Feekes scale. *Plant Pathology* **3**, 128–9.

Minogue KP, Fry WE, 1983. Models for the spread of disease: model description. *Phytopathology* **73**, 1168–73.

Mundt CC, Brophy LS, 1988. Influence of number of host genotype units on the effectiveness of host mixtures for disease control: a modeling approach. *Phytopathology* **78**, 1087–94.

Mundt CC, Brophy LS, Kolar SC, 1996. Effect of genotype unit number and spatial arrangement on severity of yellow rust in wheat cultivar mixtures. *Plant Pathology* **45**, 215–22.

Paysour RE, Fry WE, 1983. Interplot interference: a model for planning field experiments with aerially disseminated pathogens. *Phytopathology* **73**, 1014–20.

van der Plank JE, 1948. The relation between the size of fields and the spread of diseases into them. Part I. Crowd diseases. *Empire Journal of Experimental Agriculture* **16**, 134–42.

van der Plank JE, 1949. The relation between the size of fields and the spread of diseases into them. Part II. Diseases caused by fungi with air-borne spores with a note on horizons of infection. *Empire Journal of Experimental Agriculture* **17**, 18–22.

van der Plank JE, 1960. Analysis of epidemics. In: Horsfall JG, Dimond AE, eds. *Plant Pathology. III. The Diseased Population, Epidemics and Control*. New York, USA: Academic Press, 229–89.

Sackett KE, Mundt CC, 2005a. Models for primary disease gradients of wheat stripe rust. *Phytopathology* **95**, 983–91.

Sackett KE, Mundt CC, 2005b. The effects of dispersal gradient and pathogen life cycle components on epidemic velocity in computer simulations. *Phytopathology* **95**, 992–1000.

Scherm H, 1996. On the velocity of epidemic waves in model plant disease epidemics. *Ecological Modelling* **87**, 217–22.

Scherm H, Ngugi HK, Ojiambo PS, 2006. Trends in theoretical plant epidemiology. *European Journal of Plant Pathology* **115**, 61–73.

Shrum R, 1975. Simulation of wheat stripe rust (*Puccinia striiformis* West.) using EPIDEMIC, a flexible plant disease simulator. *Progress Report of the Pennsylvania Agricultural Experiment Station* **347**, 1–68.

Soubeyrand S, Enjalbert J, Sanchez A, Sache I, 2007. Anisotropy, in density and in distance, of the dispersal of yellow rust of wheat: experiments in large field plots and estimation. *Phytopathology* **97**, 1315–24.

Strengbom J, Englund G, Erikson L, 2006. Experimental scale and precipitation modify effects of nitrogen addition on a plant pathogen. *Journal of Ecology* **94**, 227–33.

Waggoner PE, 1962. Weather, space, time and chance of infection. *Phytopathology* **52**, 1100–8.

Zadoks JC, 2001. Plant disease epidemiology in the twentieth century: a picture by means of selected controversies. *Plant Disease* **85**, 808–15.

Zadoks JC, Kampmeijer P, 1977. The role of crop populations and their deployment, illustrated by means of a simulator, EPIMUL76. *Annals of the New York Academy of Sciences* **287**, 164–90.